
JOURNAL OF THE AMERICAN CHEMICAL SOCIETY

Myristoylation-Induced Compaction of a Membrane-Binding Protein

Olivier Michielin,[†] Guy Vergères,[‡] and Jeremy J. Ramsden*

Contribution from the Department of Biophysical Chemistry, Biozentrum, 4056 Basel, Switzerland

Received January 25, 1999

Abstract: Accurate measurements of the association and dissociation kinetics of myristoylated and unmyristoylated forms of MARCKS-related protein using optical waveguide lightmode spectroscopy (OWLS) reveal that the enhanced association of the myristoylated form is due principally to myristoylation inducing the protein to adopt a more compact conformation, allowing enhanced packing at the membrane surface, rather than to markedly different association and/or dissociation kinetics. The driving force for compaction appears to be the shielding of the myristoyl moiety from unfavorable aqueous solvation.

1. Introduction

Many proteins are posttranslationally provided with an alkyl chain (myristate, palmitate, etc.).¹ Since most of them have a regulatory function involving association with lipid membranes, it is widely assumed that the role of the alkyl chain is to enhance the membrane affinity of the protein. The aim of this paper is to examine whether the assumption is justified.

A number of investigations (usually based on an assay whereby the protein is incubated with lipid vesicles and its partitioning between membrane and solution assessed) have demonstrated that alkylation does indeed enhance the amount of protein bound to the membrane.² Very recently, the kinetics of membrane association and dissociation of the native (alkylated) and dealkylated forms of a protein have been measured more accurately than is possible with the vesicle-based assay, using optical waveguide lightmode spectroscopy (OWLS).³ The OWLS measurements confirmed the earlier results insofar as more alkylated protein can indeed bind, but they further revealed that (i) the initial rate of association was barely enhanced by

alkylation (and certainly insufficiently to account for the observed enhancement of the amount bound) and (ii) dissociation followed complex, nonexponential kinetics, rendering problematical the customary application of the kinetic mass action law (KMAL) to deduce the affinity from the quotient of the association and dissociation rate coefficients.

Direct inspection of the data suggests a different interpretation: what if the myristoylated protein has a more compact conformation, allowing it to pack more densely at the surface of the membrane? Simply halving the area *a* occupied per molecule at the membrane would produce the observed enhancement of the amount bound at saturation (Figure 1), even if all of the rate coefficients remained identical. The rationale for the compaction is that the polypeptide moiety would arrange itself to shield the alkyl chain from direct, energetically unfavorable contact with the aqueous solvent.

The protein selected for this investigation was MARCKS-related protein (MRP, also called MacMARCKS or F52), a 20 kDa protein 50% closely related to MARCKS (myristoylated alanine-rich C kinase substrate), predominantly expressed in

* Author for correspondence.

[†] Present address: Laboratoire de Chimie Biophysique, Institut Le Bel, 4 rue Blaise Pascal, 67000 Strasbourg, France.

[‡] Present address: ZLB Zentrallaboratorium Blutspendedienst SRK Wankdorfstrasse 10, 3000 Bern 22, Switzerland.

(1) Magee, A. I. *J. Cell Sci.* **1990**, *97*, 581–584; Casey, P. *Science* **1995**, *268*, 221–225; Bhatnagar, R. S.; Gordon, J. I. *Trends Cell Biol.* **1997**, *7*, 14–20.

(2) Vergères, G.; Ramsden, J. J. *Biochem. J.* **1998**, *330*, 5–11.

(3) Michielin, O.; Ramsden, J. J.; Vergères, G. *Biochim. Biophys. Acta* **1998**, *1375*, 110–116.

(4) Blackshear, P. J. *J. Biol. Chem.* **1993**, *268*, 1501–1504; Aderem, A. *Cell* **1992**, *71*, 713–716; Li, J.; Aderem, A. *Cell* **1992**, *70*, 791–801; Lobach, D. F.; Rochelle, J. M.; Watson, M. L.; Seldin, M. F.; Blackshear, P. J. *Genomics* **1993**, *17*, 194–204.

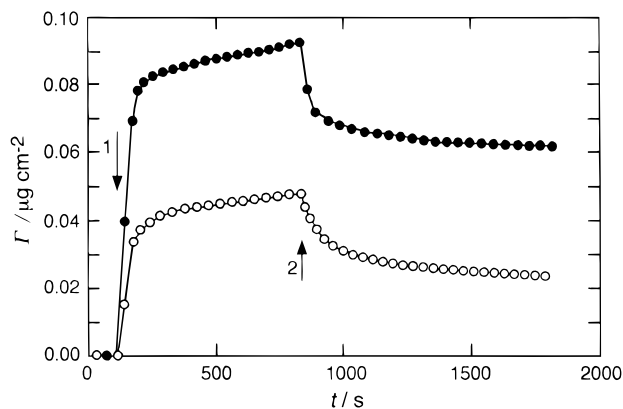


Figure 1. The binding of myr (●) and unmyr (○) MRP ($c_b = 0.2 \mu\text{M}$) to a POPC/POPG (4:1) bilayer. Arrow 1: initiation of protein flow; arrow 2: reversion to pure buffer flow.

brain and reproductive tissues,⁴ and believed to be essential for brain development and postnatal survival.⁵ It appears to have a flexible conformation in the native state.

2. Experimental Section

Proteins and Reagents. Unmyristoylated mouse MRP (unmyr) was expressed in *Escherichia coli* and purified as described previously.⁶ The N-terminal glycine residue was myristoylated cotranslationally using *N*-myristoyl transferase (NMT),⁶ yielding the myristoylated form (myr). Proteins were stored in buffer A (10 mM 3-(*N*-morpholino)propanesulfonic acid–NaOH (MOPS), pH 7.4, plus 0.1 mM EGTA) at -80°C . In all our work with the protein, we found no evidence for any degradation due to purification and storage.

Lipid Bilayer-Coated Optical Waveguides. Planar optical waveguides incorporating a grating coupler (grating constant $\Lambda = 416.15 \text{ nm}$) were obtained from Artificial Sensing Instruments (Zurich, Switzerland). They consisted of a thin (180 nm), high refractive index (1.8) layer of $\text{Si}_{0.42}\text{Ti}_{0.38}\text{O}_2$ supported on an optical glass slide. The waveguides were soaked overnight in buffer B (10 mM MOPS, pH 7.4, plus 0.1 mM EGTA and 0.1 M NaCl). To deposit a lipid bilayer membrane onto the waveguides, lipid monolayers composed of 1-palmitoyl-2-oleoyl-*sn*-glycero-3-phosphatidylcholine (POPC) and 1-palmitoyl-2-oleoyl-*sn*-glycero-3-phosphatidylglycerol (POPG),⁷ obtained from Avanti Polar Lipids (Alabaster, AL), were mixed in the molar ratio 4:1,⁶ compressed on a laboratory-built Langmuir trough filled with buffer A to a surface pressure of 32 mN/m, the so-called bilayer equivalence pressure,⁸ and transferred using a combination of vertical (Langmuir–Blodgett) and horizontal (Langmuir–Schaefer) movements.⁹ Only bilayers for which the transfer ratio of each monolayer was 1.0 were used. As a check for the possible presence of unannealed nanodefects, the tryptic fragment (i.e., lacking a transmembrane domain) of cytochrome *b5*, a small (17 kDa) protein with the same isoelectric point (4.4) as MRP, was used as a probe. It is known to adsorb to the uncoated waveguides,¹⁰ but we found it does not bind at all to POPC:POPG membranes.

Optical Waveguide Lightmode Spectroscopy (OWLS). Membrane-coated waveguides were mounted in the measuring head of an IOS-1 integrated optics scanner (Artificial Sensing Instruments, Zurich),¹¹ with which the effective refractive indices of two guided modes, the zeroth order transverse electric (TE) and transverse magnetic (TM) modes,

(5) Wu, M.; Chen, D. F.; Sasaoka, T.; Tonegawa, S. *Proc. Natl. Acad. Sci. U.S.A.* **1996**, *93*, 2110–2115; Stumpo, D. J.; Bock, C. B.; Tuttle, J. S.; Blackshear, P. J. *Proc. Natl. Acad. Sci. U.S.A.* **1995**, *92*, 944–948.

(6) Vergères, G.; Manenti, S.; Weber, T.; Stürzinger, C. *J. Biol. Chem.* **1995**, *270*, 19879–19887.

(7) Substitution of POPG by 1-palmitoyl-2-oleoyl-*sn*-glycero-3-phosphatidylserine (POPS) gave indistinguishable results.

(8) Marsh, D. *Biochim. Biophys. Acta* **1996**, *1286*, 183–223.

(9) Ramsden, J. J. *Philos. Mag. B* **1999**, *79*, 381–386.

(10) Ramsden, J. J.; Roush, D. J.; Gill, D. S.; Kurrat, R.; Willson, R. C. *J. Am. Chem. Soc.* **1995**, *117*, 8511–8516.

(11) Tiefenthaler, K. *Adv. Biosensors* **1992**, *2*, 261–289.

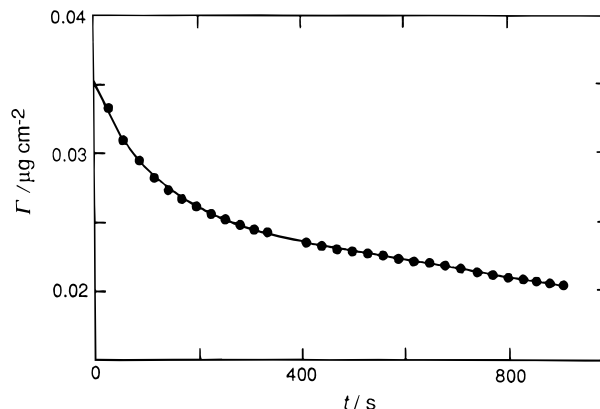


Figure 2. Desorption of bound unmyr MRP (Figure 1) while flushing with pure buffer. The solid line is the best fit of eq 1 to the data (see text). A single-exponential decay was not able to fit the data satisfactorily.

could be measured rapidly and repeatedly. A flow-through cuvette (diameter 9 mm, height 0.31 mm) was sealed with an “o”-ring onto the lipid-coated waveguide surface. Initially, pure buffer B flowed over the membrane to establish a baseline, and then the protein dissolved in buffer B at three different bulk solution protein concentrations, c_b , namely 0.2, 0.6, and $1.8 \mu\text{M}$ (4.2 , 12.6 , and $37.8 \mu\text{g}/\text{cm}^3$), and last pure buffer B again. Solution flow was controlled by a high-precision mechanical syringe pusher delivering $2.14 \text{ mm}^3/\text{s}$. The temperature of the measuring head was maintained at $25.0 \pm 0.2^\circ\text{C}$. From the two effective refractive indices the amount, Γ , of bound protein per unit area was calculated with an uncertainty of $\pm 0.2 \text{ fmol MRP}/\text{mm}^2$.^{10,12,13}

3. Results and Discussion

Dissociation. The dissociation could not be well fitted to a single exponential, but could be fitted very satisfactorily to a double exponential, i.e.,

$$\Gamma(t) = \Gamma_0 [f \exp(-k_{-1}t) + (1 - f) \exp(-k_{-2}t)] \quad (1)$$

where Γ_0 is the amount of membrane-bound protein at the onset of the pure dissociation phase ($t = 0$) and f is the fraction of MRP desorbing with rate coefficient k_{-1} , the other rate coefficient being k_{-2} . All our dissociation curves could be fitted by eq 1 (an example is shown in Figure 2), and the corresponding values of k_{-1} and k_{-2} are given in Table 1.

The existence of two desorption processes implies two distinct populations of MRP bound to the membrane. In analogy to the behavior of cytochrome *b5* binding to lipid vesicles,¹⁴ we refer to the population which desorbs with the faster rate coefficient (k_{-1}) as the “loose” (i.e., loosely bound) conformation (L), and the population which desorbs with the slower rate coefficient (k_{-2}) as the “tight” (tightly bound) conformation (T).

Association. Given the above evidence for two types of membrane-associated MRP, we propose that MRP present in the bulk (MRP_b) binds initially to the membrane in the loose conformation, which changes into the tight conformation at the membrane in a first-order process characterized by a rate coefficient k_2 . The complete reaction scheme is therefore

(12) Ramsden, J. J. *J. Stat. Phys.* **1993**, *73*, 853–877.

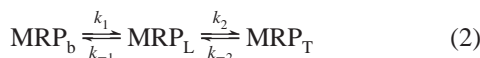
(13) The refractive index increment of the protein was taken to be $0.18 \text{ cm}^3/\text{g}$.

(14) When added to large preformed vesicles, cytochrome *b5* binds loosely, as characterized by the fact that it can be transferred to other vesicles; when added to small vesicles or incorporated into vesicles by the detergent-dialysis technique, it binds tightly and cannot be thus transferred.¹⁵

Table 1. Parameters Obtained by Fitting the Sum of Integrated Eqs 4 and 5 to the Data using the ASIEVAL Software written by R. Kurrat^a

parameter	unmyr MRP	myr MRP	myr/unmyr
$k_1/(10^4 \times \text{M}^{-1} \text{s}^{-1})$	2.3 ± 0.2	3.5 ± 0.3	1.5
$k_{-1}/(10^{-2} \times \text{s}^{-1})$	1.5 ± 0.2	2.6 ± 0.8	1.7
$k_2/(10^{-3} \times \text{s}^{-1})$	2.1 ± 0.3	1.2 ± 0.3	0.6
$k_{-2}/(10^{-4} \times \text{s}^{-1})$	3.0 ± 0.6	0.6 ± 0.1	0.2
$K_L/(10^6 \times \text{M}^{-1})$	1.5 ± 0.2	1.3 ± 0.4	0.9
$K/(10^7 \times \text{M}^{-1})$	1.2 ± 0.3	5.8 ± 1.2	4.8
a/nm^2	17.0 ± 1.7	10.7 ± 1.7	0.6

^a K characterizes the overall affinity of MRP for the membrane and is defined by $K = k_1(k_2 + k_{-2})/(k_{-1}k_{-2})$; K_L is an apparent association constant characterizing the affinity of the loose conformation for the planar bilayer and is defined as $K_L = k_1/k_{-1}$. a is the area occupied per adsorbed molecule. The adsorption rate coefficient k_1 has been converted from the heterogeneous units (cm/s) implied by eq 5 to homogeneous ones ($\text{M}^{-1} \text{s}^{-1}$) by multiplying by $aN_A/1000$, where N_A is Avogadro's number. Uncertainties give the range over the entire data set.



and the corresponding kinetic equations are

$$d\Gamma_L/dt = k_1c_b - k_{-1}\Gamma_L + k_{-2}\Gamma_T - k_2\Gamma_L \quad (3)$$

and

$$d\Gamma_T/dt = k_2\Gamma_L - k_{-2}\Gamma_T \quad (4)$$

where Γ_L and Γ_T are the respective amounts of MRP_L and MRP_T at the membrane surface, their sum $\Gamma = \Gamma_L + \Gamma_T$ being the actual quantity determined experimentally. Hence, the kinetic traces should be fitted by integrating eqs 3 and 4.¹⁶ Since k_{-1} and k_{-2} are determined from separate analyses of the dissociation alone and the lower limit of k_1 is fixed by $(d\Gamma/dt)_{t=0} \leq k_1c_b$ which can be estimated directly from the data, the only fully adjustable parameter is k_2 . With this procedure it was impossible to obtain satisfactory fits (Figure 3, long dashes). The constraints on k_1 , k_{-1} , and k_{-2} imply that significantly higher amounts of protein should be deposited on the membrane than those actually measured.

To resolve this apparent paradox we have to consider that eq 3 does not account for the fact that at most a single monolayer of MRP can bind to the membrane, which will therefore be gradually filled up and this feature must be included in the association kinetics. Let the function $\phi(\Gamma)$ give the probability that a protein arriving at the membrane will find a vacant region large enough for it to bind. At the start of adsorption $\phi = 1$, and binding ceases when $\phi = 0$. For adsorption onto a continuum, ϕ can be expanded in powers of the occupied fraction θ of the surface (defined as $\theta = \Gamma a/m$, where $m (= 3.33 \times 10^{-14} \mu\text{g})$ is the mass of a single MRP molecule).¹⁸ We used the accurate interpolation formula,¹⁹

$$\phi = (1 - \bar{\theta})^3 / (1 - b_1\bar{\theta} + b_2\bar{\theta}^2 - b_3\bar{\theta}^3 + b_4\bar{\theta}^4)$$

(15) Vergères, G.; Waskell, L. *Biochimie* **1995**, *77*, 604–620.

(16) Strictly speaking, in eq 3 we should write not c_b , but c_v , the concentration of MRP in the immediate vicinity of the surface, and complement eqs 3 and 4 by a third equation giving the rate of change of c_v .¹⁷ We found, however, that c_v deviates significantly from c_b only at the very beginnings of the adsorption and desorption phases, and hence neglect the deviation.

(17) Ramsden, J. J. In *Biopolymers at Interfaces*; Malmsten, M., Ed.; Dekker: New York, 1998; Chapter 10.

(18) Schaaf, P.; Talbot, J. J. *Chem. Phys.* **1989**, *91*, 4401–4409.

(19) Jin, X.; Talbot, J.; Wang, N.-H. L. *AIChE J.* **1994**, *40*, 1685–1696.

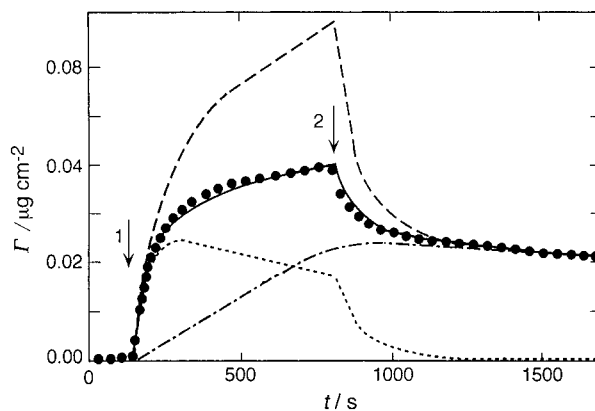


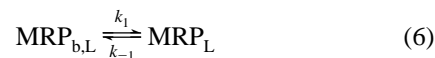
Figure 3. Measured binding of unmyr MRP (\bullet , $c_b = 0.2 \mu\text{M}$) to a POPC/POPG (4:1) bilayer. Arrows 1 and 2 indicate respectively the initiations of protein and buffer flows. Long dashes, predicted association and dissociation of unmyr MRP using eqs 3 and 4 with k_{-1} and k_{-2} predetermined by fitting eq 1 to the dissociation part only (following arrow 2). Solid line: Fit of eqs 4 and 5 to the data (see parameters in Table 1), again with k_{-1} and k_{-2} predetermined from eq 2. All three concentrations could be fitted with the same parameters (i.e., only c_b was changed). The short dashed and dashed-dotted lines show the calculated amounts of the L and T forms, respectively.

where b_1 (0.8237), b_2 (0.458), b_3 (0.67), and b_4 (0.87) are empirical constants and $\bar{\theta} = \theta/\theta_j$, with θ_j being the fractional surface coverage at which deposition of a particle becomes sterically impossible, i.e., at which $\phi = 0$ (the so-called jamming limit). It was put equal to 0.55 since this value is valid for spheres as well as for rodlike particles with an axial ratio of 4.^{20,21} Hence, we can replace eq 3 by

$$d\Gamma_L/dt = k_1c_b\phi - k_{-1}\Gamma_L + k_{-2}\Gamma_T - k_2\Gamma_L \quad (5)$$

The incorporation of the available area function ϕ allowed the data to be fitted satisfactorily (Figure 3, solid line), with a as an additional free parameter. The same parameters (except for c_b) could be used for all of the different bulk concentrations investigated, provided that the protein was of the same type (myr or unmyr). Hence we ended up with two sets of parameters, which are collected in Table 1.

Fitting Other Models. We also investigated a parallel model in which L and T are preformed in the bulk solution and bind independently to the membrane, that is,



and



The experimental data could be fitted equally satisfactorily to the equations describing this scheme. The fitted values of k_{-1} , k_{-2} , and a were identical to those obtained with the first scheme, and the values of k_1 and k_2 were somewhat different. We do not favor this scheme on independent grounds, however, since no other results have revealed multiple protein types in solution in the concentration range used in our studies.

Significance of the Parameters. Association of myr is slightly faster than unmyr, but this is compensated for by faster

(20) Viot, P.; Tarjus, G.; Ricci, S. M.; Talbot, J. J. *Chem. Phys.* **1992**, *97*, 5212–5218.

(21) Schleiff, E.; Schmitz, A.; McIlhinney, R. A. J.; Manenti, S.; Vergères, G. *J. Biol. Chem.* **1996**, *271*, 26794–26802.

dissociation of L, hence within experimental uncertainty *its formal affinity* K_L is the same. Conversion to T is about twice as fast for myr compared with unmyr, but its dissociation is 5 times slower, resulting in the overall affinity (K) of myr being about 5-fold greater than that of unmyr.

Strikingly, the area per molecule of unmyr is almost double that of myr, and *it is this difference which is primarily responsible for the significantly greater amounts of myr bound compared with amounts of unmyr.*

Energetics of Association. The difference $\Delta\Delta G$ between myr and unmyr equals RT times the natural logarithm of the ratio of the affinities. Since the ratio of the K_L is practically unity, it can be inferred that the myristate group does not confer any enhanced membrane affinity to the protein bound in the loose form. It has, however, been demonstrated that the myristate does ultimately insert into the membrane,⁶ the energetic contribution of which is given by the ratio of the K , i.e., $\Delta\Delta G \approx 4$ kJ/mol.

In inferring affinities from rate coefficients (i.e., making use of the KMAL) it should be borne in mind that our k_1 subsumes the diffusion coefficient D of the protein as well as the interfacial (protein–membrane) energetics.^{10,17} D is inversely proportional to the hydrodynamic radius of the protein in solution. If the smaller a (corresponding to myr) reflects a more compact conformation of the dissolved protein, then D should be inversely proportional to \sqrt{a} , implying that the ratio $k_{1,\text{myr}}/k_{1,\text{unmyr}}$ should equal $(a_{\text{unmyr}}/a_{\text{myr}})^{1/2}$. From Table 1, the ratio of the k_1 is 1.5 ± 0.2 , and the ratio of \sqrt{a} is 1.3 ± 0.1 , in agreement with the postulate. We attempted to corroborate our values of a by estimating D from analytical ultracentrifugation (AU). Results from unmyr were consistent with an elongated form (axial ratio estimated at between 7 and 12, depending on the supposed degree of hydration of the protein²¹). The surface occupied (projected area) by such a prolate molecule lying with its long axis parallel to the membrane falls in the range 19–24 nm², in agreement with our determination of a from the binding kinetics.

It may seem counterintuitive that myr dissociates from the membrane in its L form more rapidly than unmyr, but of course it is undesirable for L to accumulate, since it blocks occupation by T, which, we may suppose, is the one required for signal transduction by MRP. Hence rapid dissociation of L actually accelerates occupation by T. A measure of this process is the kinetic efficiency parameter τ defined previously²²

$$\tau = k_{-2}/(k_{-1}k_2) \quad (8)$$

The shorter this time, the faster T will be accumulated. From the data in Table 1, we compute $\tau(\text{unmyr}) = 9.5$ s, whereas $\tau(\text{myr})$ is only 1.9 s.

4. Conclusions

The main effect of myristoylation is to induce a more compact form of MRP, which allows, *inter alia*, more protein to be accumulated at the membrane. Compaction of the myristoylated protein in solution is likely to reflect conformational rearrangement to minimize exposure of the myristoyl moiety to water.

The molecular interpretation of the loosely and tightly bound membrane states is that the protein is peripherally associated with, but not inserted into, the membrane in the former state. Conversion to the latter requires conformational rearrangement, possibly to enable hydrophobic side chains and in the case of myr, the myristoyl moiety, to insert into the membrane. That $k_{2,\text{myr}} < k_{2,\text{unmyr}}$ reflects the fact that this rearrangement is more extensive in the case of myr than for unmyr.

A final conclusion concerns the value of the methodology adopted in this paper to deduce structural information about a protein. Conventional approaches (X-ray diffraction, nuclear magnetic resonance) have been tried without success with MARCKS and MRP. The circular dichroism of both MARCKS²³ and MRP²¹ are consistent with the protein being a random coil in solution. Other techniques such as analytical ultracentrifugation and quasi-elastic light scattering require protein concentrations at least an order of magnitude greater than the highest concentration we have used (which already probably exceeds the concentrations prevailing *in vivo*, i.e., in the cytoplasm) and one cannot extrapolate from the high concentrations to the lower ones without demonstrating that the state of the protein is the same in both, especially since proteins with affinity for lipid membranes are necessarily amphiphilic, making them prone to aggregation (micellization) at high concentrations. Moreover, these techniques only yield information on the solution form of the protein, whereas our goal is to investigate what happens to the protein at the solution/membrane interface. From an analysis of the kinetic adsorption data, we have been able to reliably deduce the area occupied per molecule, as well as the association and dissociation rate coefficients and hence the affinities.

Acknowledgment. We thank Christoph Stürzinger for having purified MRP, Perry Blackshear (Duke University Medical Center, Durham, North Carolina) for the plasmid pET3dF52M1 containing the MRP gene, Jeffrey Gordon (Washington University, School of Medicine, St. Louis, Missouri) for the plasmid pBB131NMT containing the gene coding for *N*-myristoyl transferase used to myristoylate the polypeptide, and Roger Kurrat (ETH Zurich) for having written the software used to fit the equations to the data. GV thanks the Swiss National Science Foundation for financial support (Grant No. 3100-042045.94 to G. Schwarz), and J.J.R. thanks the Ciba-Geigy-Jubiläums-Stiftung.

JA990239J

(22) Ramsden, J. J.; Bachmanova, G. I.; Archakov, A. I. *Biosens. Bioelectron.* **1996**, *11*, 523–528.

(23) Manenti, S.; Sorokine; Van Dorsselaer, A.; Taniguchi, H. *J. Biol. Chem.* **1992**, *267*, 22310–22315.